

Can Large Language Models Improve Spectral Graph Neural Networks?

Kangkang Lu¹, Yanhua Yu¹, Zhiyong Huang², Tat-Seng Chua²

¹Beijing University of Posts and Telecommunications

²National University of Singapore

lukangkang@bupt.edu.cn, yuyanhua@bupt.edu.cn, dcshuang@nus.edu.sg, dcscts@nus.edu.sg

Abstract

Spectral Graph Neural Networks (SGNNs) have attracted significant attention due to their ability to approximate arbitrary filters. They typically rely on supervision from downstream tasks to adaptively learn appropriate filters. However, under label-scarce conditions, SGNNs may learn suboptimal filters, leading to degraded performance. Meanwhile, the remarkable success of Large Language Models (LLMs) has inspired growing interest in exploring their potential within the GNN domain. This naturally raises an important question: *Can LLMs help overcome the limitations of SGNNs and enhance their performance?* In this paper, we propose a novel approach that leverages LLMs to estimate the homophily of a given graph. The estimated homophily is then used to adaptively guide the design of polynomial spectral filters, thereby improving the expressiveness and adaptability of SGNNs across diverse graph structures. Specifically, we introduce a lightweight pipeline in which the LLM generates homophily-aware priors, which are injected into the filter coefficients to better align with the underlying graph topology. Extensive experiments on benchmark datasets demonstrate that our LLM-driven SGNN framework consistently outperforms existing baselines under both homophilic and heterophilic settings, with minimal computational and monetary overhead.

1 Introduction

The past decade has witnessed great success and prosperity of graph neural networks (GNNs) in diverse data science and engineering scenarios, such as traffic network (Hu et al. 2019; Jiang and Luo 2022), abnormal detection (Tang et al. 2022, 2024a), relational databases (Cappuzzo, Papotti, and Thirumuruganathan 2020; Huang et al. 2022) and recommender systems (Sharma et al. 2024; Gao et al. 2023). Existing GNNs can be broadly categorized into spatial GNNs and spectral GNNs. Spatial GNNs often adopt a message-passing mechanism to learn node representations by aggregating neighbor node features. In contrast, spectral GNNs map node features to a new desired space by selectively attenuating or amplifying the Fourier coefficients induced by the normalized Laplacian matrix. This study primarily centers on the realm of spectral GNNs.

In real-world scenarios, graphs often exhibit varying degrees of homophily. In homophilic graphs, nodes of the same class are more likely to be connected, whereas in het-

erophilic graphs, connections tend to form between nodes of different classes. Prior studies [24, 37, 42] have shown that heterophilous structures pose significant challenges for spatial GNNs based on message passing, as these models typically rely on the implicit assumption of homophily. To address this issue, many methods have been proposed from the spatial perspective [40]. In contrast, spectral GNNs [3, 19] with learnable filters offer a promising alternative. By learning spectral filters directly from the graph structure, these models can better adapt to heterophilic settings and mitigate the aggregation of noisy information from dissimilar neighbors.

However, since the labels of real-world graph datasets may be very sparse, existing spectral graph neural network methods will learn inappropriate filters, resulting in suboptimal performance. As shown in Figure 1, the optimal filter on the Cora dataset is a low-pass filter due to its high homophily. However, classical spectral graph neural networks such as GPRGNN (Chien et al. 2021), BernNet (He et al. 2021), and JacobiConv (Wang and Zhang 2022) learn high-pass filters. Therefore, the performance of spectral graph neural networks may be suboptimal.

In recent years, large language models (LLMs), exemplified by GPT-4 (Achiam et al. 2023), have shown impressive proficiency in comprehending and reasoning over textual information, thereby revolutionizing a wide range of domains, including natural language processing (Zhao et al. 2023), computer vision (Wu et al. 2023), and graph representation learning (Ren et al. 2024)]. In this work, we explore the potential of language models in spectral graph neural networks. To the best of our knowledge, this is the first study to leverage large language models to improve spectral graph neural networks. Specifically, we aim to address the following research questions:

1. Can large language models (LLMs) enhance spectral GNNs? LLMs are well known for their prowess in understanding natural language, while spectral GNNs excel at node classification in heterophilic graphs. Effectively combining the text comprehension capabilities of LLMs with the filtering power of spectral GNNs presents a significant challenge. Existing efforts to integrate GNNs and LLMs typically take one of two approaches: either feeding textual graphs directly into LLMs—limiting the model’s ability to leverage graph structure, or fine-tuning LLMs for graph-

specific tasks, which introduces substantial computational and deployment costs.

2. Can LLMs effectively guide and be integrated into existing spectral GNNs? Spectral GNNs have the powerful ability to approximate arbitrary filters, which are particularly suitable for both homophilic and heterophilic graphs. However, these models usually rely on supervision from downstream tasks to learn appropriate spectral filters, which can lead to suboptimal filter learning in label-scarce or weakly-supervised settings. On the other hand, LLMs demonstrate strong performance in language understanding and text-driven tasks, as seen in models like LLM-GNN (Chen et al. 2023b). This opens up a promising and novel direction: using LLM-generated predictions to assist and improve spectral GNNs.

In this paper, we propose an LLM-based enhancement framework for spectral GNNs. Specifically, to address the first research question: spectral GNNs may learn inappropriate filters due to sparse labels, while the homophily ratio serves as a global characteristic of a graph dataset. We naturally leverage LLMs to predict the homophily ratio, enabling spectral GNNs to perceive global graph properties even under limited supervision. Notably, predicting homophily only requires sampling around 100 edges, making the cost per dataset as low as \$1, without the need for costly fine-tuning or deployment.

For the second research question, we incorporate the predicted homophily ratio into existing polynomial spectral GNNs to enhance their performance. Specifically, we construct various heterophily-aware bases according to the predicted homophily, and then integrate them into polynomial spectral GNNs. This integration allows the model to fully utilize homophily information, boosting overall performance.

Our contributions are summarized as follows:

- To the best of our knowledge, this is the first work to investigate the integration of LLMs into spectral GNNs. We show that LLMs can effectively predict the homophily ratio to guide spectral GNNs, thereby boosting their performance without the need for fine-tuning or additional deployment overhead.
- We introduce a novel LLM-based enhancement framework for spectral GNNs, which is compatible with various LLMs and polynomial spectral architectures. By leveraging the global semantic understanding of LLMs, our method significantly improves the adaptability and performance of spectral GNNs across diverse scenarios.
- Extensive experiments on multiple benchmark datasets demonstrate that our method consistently improves the performance of existing spectral GNNs, while incurring minimal computational and financial overhead.

2 Related Work

This section introduces related research, including spectral GNNs and LLM for Graph.

Spectral GNNs. According to whether the filter can be learned, the spectral GNNs can be divided into *pre-defined filters* and *learnable filters*. In the category of pre-defined

filters, GCN (Kipf and Welling 2017) uses a simplified first-order Chebyshev polynomial. APPNP (Gasteiger, Bojchevski, and Günnemann 2019) utilizes Personalized Page Rank to set the weight of the filter. In the category of learnable filters, ChebNet (Defferrard, Bresson, and Vandergheynst 2016) uses Chebyshev polynomials with learnable coefficients. GPR-GNN (Chien et al. 2021) extends APPNP by directly parameterizing its weights. BernNet (He et al. 2021) uses Bernstein polynomials to learn filters and forces all coefficients positive. JacobiConv (Wang and Zhang 2022) adopts an orthogonal and flexible Jacobi basis to accommodate a wide range of weight functions. ChebNetII (He, Wei, and Wen 2022) uses Chebyshev interpolation to learn filters. Specformer (Bo et al. 2023) performs self-attention in the spectral domain to learn a set-to-set spectral filter. Recently, some works have applied spectral GNNs to node-level filtering. For example, DSF (Guo et al. 2023) proposes a novel diversified spectral filtering framework that automatically learns node-specific filter weights. UniFilter (Huang et al. 2024) integrates heterophilic and homophilic bases to construct a universal polynomial basis, UniBasis, which partially alleviates the problems of over-smoothing and over-squashing.

LLM for Graph. Existing research on applying large language models (LLMs) to graph learning can be broadly categorized into GNN-centric and LLM-centric approaches. GNN-centric methods leverage LLMs to extract node features from raw data, and then use GNNs for downstream prediction tasks (He et al. 2024; Xie et al. 2023). In contrast, LLM-centric methods integrate GNNs to enhance the performance of LLMs in graph-related tasks (Tang et al. 2024b; Zhang et al. 2024a). Some studies also employ LLMs to assign edge weights in text-attributed graphs (Sun et al. 2023; Ling et al. 2024). However, these methods are not specifically designed for heterophilic graphs. Beyond these, a few studies aim to enhance GNNs by leveraging LLMs to identify meaningful or noisy edges. For instance, GraphEdit (Guo et al. 2024) utilizes LLMs for graph structure learning by detecting and removing noisy connections; LLM4RGNN (Zhang et al. 2024b) identifies malicious and critical edges to improve the adversarial robustness of GNNs; and LLM4HeG (Wu et al. 2024) integrates LLMs into GNNs for heterophilic TAGs through edge discrimination and adaptive edge reweighting.

In contrast to existing methods, the proposed method uniquely focuses on leveraging LLMs to improve and enhance spectral GNNs, which has been underexplored in prior work.

3 Preliminaries

3.1 Spectral GNN

Assume we are given an undirected homogeneous graph $\mathcal{G} = (\mathcal{V}, \mathcal{E}, \mathbf{X})$, where $\mathcal{V} = \{v_1, \dots, v_n\}$ denotes the set of n nodes, \mathcal{E} is the edge set, and $\mathbf{X} \in \mathbb{R}^{n \times d}$ is the node feature matrix. The corresponding adjacency matrix is $\mathbf{A} \in \{0, 1\}^{n \times n}$, where $\mathbf{A}_{ij} = 1$ if there is an edge between nodes v_i and v_j , and $\mathbf{A}_{ij} = 0$ otherwise. The degree matrix $\mathbf{D} = \text{diag}(d_1, \dots, d_n)$ is a diagonal matrix where the

i -th diagonal entry is $d_i = \sum_j \mathbf{A}_{ij}$. The normalized Laplacian matrix is defined as $\hat{\mathbf{L}} = \mathbf{I} - \mathbf{D}^{-\frac{1}{2}} \mathbf{A} \mathbf{D}^{-\frac{1}{2}}$, where \mathbf{I} denotes the identity matrix. The normalized adjacency matrix is $\hat{\mathbf{A}} = \mathbf{D}^{-\frac{1}{2}} \mathbf{A} \mathbf{D}^{-\frac{1}{2}}$. Let $\hat{\mathbf{L}} = \mathbf{U} \mathbf{\Lambda} \mathbf{U}^\top$ denote the eigen-decomposition of $\hat{\mathbf{L}}$, where \mathbf{U} is the matrix of eigenvectors and $\mathbf{\Lambda} = \text{diag}([\lambda_1, \lambda_2, \dots, \lambda_n])$ is the diagonal matrix of eigenvalues.

Spectral GNNs are based on the Fourier transform in signal processing. The Fourier transform of a graph signal \mathbf{x} is given by $\hat{\mathbf{x}} = \mathbf{U}^\top \mathbf{x}$, and its inverse is $\mathbf{x} = \mathbf{U} \hat{\mathbf{x}}$. Accordingly, the graph convolution of the signal \mathbf{x} with a kernel \mathbf{g} can be defined as:

$$\mathbf{z} = \mathbf{g} *_{\mathcal{G}} \mathbf{x} = \mathbf{U} ((\mathbf{U}^\top \mathbf{g}) \odot (\mathbf{U}^\top \mathbf{x})) = \mathbf{U} \hat{\mathbf{G}} \mathbf{U}^\top \mathbf{x}, \quad (1)$$

where $\hat{\mathbf{G}} = \text{diag}(\hat{g}_1, \dots, \hat{g}_n)$ denotes the spectral kernel coefficients. To avoid explicit eigen-decomposition, recent works approximate different kernels \mathbf{H} using polynomial functions $h(\cdot)$ as follows:

$$\mathbf{H} = h(\hat{\mathbf{L}}) = h_0 \hat{\mathbf{L}}^0 + h_1 \hat{\mathbf{L}}^1 + h_2 \hat{\mathbf{L}}^2 + \dots + h_K \hat{\mathbf{L}}^K, \quad (2)$$

where K is the order of the polynomial $h(\cdot)$ and h_K is the coefficient of the K -th order term. Thus, Eq. (1) can be rewritten as:

$$\mathbf{Z} = \mathbf{H} \mathbf{X} = h(\hat{\mathbf{L}}) \mathbf{X} = \mathbf{U} h(\mathbf{\Lambda}) \mathbf{U}^\top \mathbf{X}, \quad (3)$$

where \mathbf{Z} is the output (prediction) matrix. According to Eq. (2), Eq. (3), and recent studies (Chen et al. 2023a), a K -th order polynomial in spectral GNNs is equivalent to aggregating information from K -hop neighbors in spatial GNNs.

3.2 Homophily

The homophily metric measures the degree of association between connected nodes. Homophily can be measured in various ways, such as node-level homophily, edge-level homophily, and class-level homophily. The widely adopted edge homophily (Zhu et al. 2020) is defined as follows:

$$\mathcal{H}_{\text{edge}}(\mathcal{G}) = \frac{1}{|\mathcal{E}|} \sum_{(u,v) \in \mathcal{E}} \mathbf{1}(y_u = y_v), \quad (4)$$

where $\mathbf{1}(\cdot)$ is the indicator function, i.e., $\mathbf{1}(\cdot) = 1$ if the condition holds, otherwise $\mathbf{1}(\cdot) = 0$. y_u is the label of node u , and y_v is the label of node v . $|\mathcal{E}|$ is the size of the edge set.

4 Methodology

This section describes the proposed method, which consists of two modules: (1) using an LLM to predict the homophily, and (2) incorporating the predicted homophily into existing spectral GNNs. The following provides a detailed introduction to these two modules.

4.1 Estimating Homophily Using LLM

It is well established that, for a graph, the homophily ratio measures the degree of correlation among neighboring nodes and reflects the proportion of edges connecting nodes of the same class. Consequently, accurately estimating the homophily ratio is critical for better leveraging the graph’s structural properties and enabling targeted spectral filtering. For example, in a highly homophilic graph, a polynomial spectral GNN should ideally learn a low-pass filter.

Table 1: Comparison of homophily predicted by the LLM with varying prompts, with indicators for whether CoT and Most-voting are used.

Prompt Type		Cora	Citeseer	Pubmed	History
CoT	Most-voting				
×	×	0.41	0.63	0.72	0.58
✓	×	0.51	0.76	0.67	0.65
×	✓	0.37	0.63	0.81	0.55
✓	✓	0.70	0.81	0.83	0.77
Ground Truth		0.81	0.78	0.80	0.66

For simplicity, we adopt the widely used edge-level homophily as our estimation target, as Eq. (4). Specifically, we aim to estimate the proportion of homophily edges (i.e., edges linking nodes of the same class) among all edges. However, it is impractical to evaluate the homophily of every edge, especially in large-scale graphs with millions of edges, due to the high inference cost associated with LLMs. Therefore, we propose to estimate the overall homophily ratio by sampling a subset of edges.

To achieve accurate estimation of the homophily ratio, it is important to assess the reliability of predictions, such as through calibrated confidence scores. Motivated by recent advances (Chen et al. 2023b) in generating calibrated confidence from LLMs, we investigate the following strategies:

- **Vanilla prompting:** Directly querying the model for its confidence.
- **Reasoning-based prompting (CoT):** Guiding the model through annotation generation using techniques such as chain-of-thought and multi-step reasoning.
- **Consistency-based prompting (Most-voting):** Querying the model multiple times and selecting the most frequent prediction via majority voting.
- **Hybrid prompting:** Combining Reasoning-based and consistency-based methods to enhance robustness.

As shown in Table 1, both reasoning-based prompting and consistency-based prompting contribute to improved performance in predicting homophily. Therefore, we adopt a hybrid prompting strategy that integrates their respective strengths to further enhance the accuracy of homophily estimation. For example, the prompt used for the Cora dataset is designed as follows, while prompts for other datasets can be found in Appendix A.

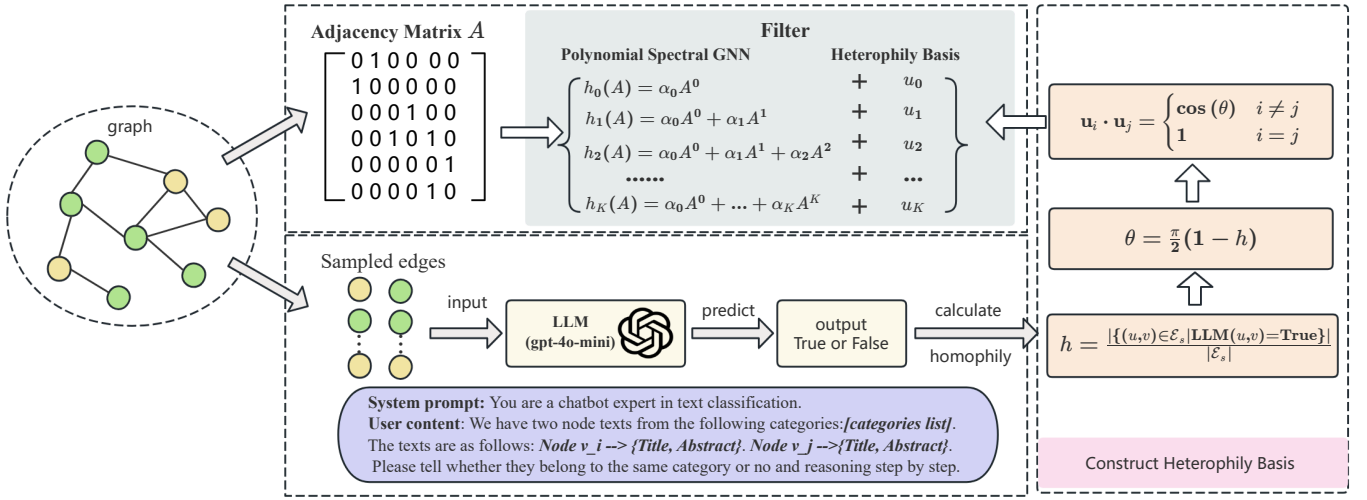


Figure 1: The overall framework of the proposed model. First, the proposed method samples a subset of edges (node pairs) from the dataset. Then we use LLM to predict whether the connected nodes belong to the same class. Based on the LLM’s predictions, we estimate the graph’s homophily. Finally, a heterophily basis is constructed using the predicted homophily and integrated into existing polynomial spectral GNNs to perform the node classification task.

System: You are a chatbot expert in text classification.
User: We have two node texts from the following 7 categories: *[categories list]*. The texts are as follows: *Node v_i → {Title, Abstract}*. *Node v_j → {Title, Abstract}*. Please tell me whether they belong to the same category or not after reasoning step by step.

After obtaining the homophily labels for a subset of edges using reasoning-based prompting, we further apply consistency-based prompting by querying each sample five times. If at least three out of five predictions yield the same answer, we consider it the final prediction for that sample. The process is illustrated as follows:

$$y_e = \begin{cases} 1 & \text{if } r_e \geq 3 \\ 0 & \text{if } r_e < 3 \end{cases},$$

Once the predictions for each sampled edge are obtained, we compute the predicted edge-level homophily \hat{h} as follows:

$$\hat{h} = \frac{|\{(u, v) \in \mathcal{E}_s \mid \text{LLM}(u, v) = \text{True}\}|}{|\mathcal{E}_s|}, \quad (5)$$

where \mathcal{E}_s denotes the set of all sampled edges.

4.2 Combination of Homophily with Existing Polynomial Filters

After predicting the homophily ratio using an LLM, we incorporate the estimated value into an existing polynomial spectral GNN. To enable spectral GNNs to leverage the homophily information predicted by Eq. (5), we construct a set of heterophily-aware basis vectors inspired by UniFilter (Huang et al. 2024). Specifically, the angle between each pair of basis vectors is defined as follows:

$$\theta = \frac{\pi}{2}(1 - \hat{h}).$$

Thus, the angle between different heterophily-aware basis vectors \mathbf{u}_i and \mathbf{u}_j is given by:

$$\mathbf{u}_i \cdot \mathbf{u}_j = \begin{cases} \cos \theta = \cos \left(\frac{(1-\hat{h})\pi}{2} \right) & \text{if } i \neq j, \\ 1 & \text{if } i = j. \end{cases}$$

After obtaining the heterophily basis vectors set $\{\mathbf{u}_0, \mathbf{u}_1, \dots, \mathbf{u}_K\}$, we incorporate them into existing polynomial spectral GNNs, such as GPRGNN (Chien et al. 2021), BernNet (He et al. 2021), and JacobiConv (Wang and Zhang 2022).

Insertion into GPR-GNN. GPR-GNN (Chien et al. 2021) directly assigns a learnable coefficient to each order of the normalized adjacency matrix $\hat{\mathbf{A}}$, and its polynomial filter is defined as:

$$\mathbf{z} = \sum_{k=0}^K \gamma_k \hat{\mathbf{A}}^k = \mathbf{U} g_{\gamma, K}(\Lambda) \mathbf{U}^T, \quad (6)$$

where $g_{\gamma, K}(\Lambda)$ is an element-wise operation, and $g_{\gamma, K}(x) = \sum_{k=0}^K \gamma_k x^k$. GPR-GNN represents the simplest form of polynomial spectral GNN, assigning a single scalar coefficient to each propagation step. Therefore, we directly incorporate heterophily basis vectors into GPR-GNN in ascending order of their polynomial order:

$$\mathbf{z} = \sum_{k=0}^K \gamma_k \left(\beta \hat{\mathbf{A}}^k \mathbf{x} + (1 - \beta) \mathbf{u}_k \right), \quad (7)$$

where β is a tunable hyperparameter.

Insertion into BernNet. BernNet (He et al. 2021) expresses the filtering operation with Bernstein polynomials and forces all coefficients to be positive, and its filter is de-

defined as:

$$\mathbf{z} = \sum_{k=0}^K \theta_k \frac{1}{2^K} \binom{K}{k} (2\mathbf{I} - \mathbf{L})^{K-k} \mathbf{L}^k \mathbf{x}. \quad (8)$$

For BernNet, each term is a product involving both $2\mathbf{I} - \mathbf{L}$ and \mathbf{L} . We insert the k -th heterophily basis vector \mathbf{u}_k into the k -th order of \mathbf{L} :

$$\mathbf{z} = \sum_{k=0}^K \theta_k [\beta \frac{1}{2^K} \binom{K}{k} (2\mathbf{I} - \mathbf{L})^{K-k} \mathbf{L}^k \mathbf{x} + (1 - \beta) \mathbf{u}_k]. \quad (9)$$

Insertion into JacobiConv. JacobiConv (Wang and Zhang 2022) proposes a Jacobi basis to adapt a wide range of weight functions due to its orthogonality and flexibility. The iterative process of the Jacobi basis can be defined as:

$$\begin{aligned} P_0^{a,b}(x) &= 1, \\ P_1^{a,b}(x) &= 0.5a - 0.5b + (0.5a + 0.5b + 1)x, \\ P_k^{a,b}(x) &= (2k + a + b - 1) \\ &\quad \cdot \frac{(2k + a + b)(2k + a + b - 2)x + a^2 - b^2}{2k(k + a + b)(2k + a + b - 2)} P_{k-1}^{a,b}(x) \\ &\quad - \frac{(k + a - 1)(k + b - 1)(2k + a + b)}{k(k + a + b)(2k + a + b - 2)} P_{k-2}^{a,b}(x), \end{aligned} \quad (10)$$

where a and b are tunable hyperparameters. Unlike GPR-GNN and BernNet, JacobiConv adopts an individual filter function for each output dimension l :

$$\mathbf{Z}_{:l} = \sum_{k=0}^K \alpha_{kl} P_k^{a,b}(\hat{\mathbf{A}})(\mathbf{X}\mathbf{W})_{:l}. \quad (11)$$

Similarly, we incorporate the corresponding heterophily basis vector \mathbf{u}_k into each polynomial order of JacobiConv as follows:

$$\mathbf{Z}_{:l} = \sum_{k=0}^K \alpha_{kl} [\beta P_k^{a,b}(\hat{\mathbf{A}})(\mathbf{X}\mathbf{W})_{:l} + (1 - \beta) \mathbf{u}_k]. \quad (12)$$

4.3 Training Objective

After integrating the LLM-estimated homophily ratio into existing polynomial spectral filters, node classification can be performed using various polynomial-based spectral GNNs. Notably, the proposed method introduces no additional trainable parameters; it simply incorporates heterophily-aware basis vectors guided by the estimated homophily.

We adopt a multi-layer perceptron (MLP) with parameter θ to predict the label distribution:

$$\hat{\mathbf{y}} = \text{MLP}(\mathbf{Z}; \theta), \quad (13)$$

where $\hat{\mathbf{y}}$ is the predicted label distribution. Then, we optimize the cross-entropy loss of the node j :

$$\mathcal{L} = \sum_{j \in \mathcal{V}_{\text{train}}} \text{CrossEntropy}(\hat{\mathbf{y}}^j, \mathbf{y}^j), \quad (14)$$

where $\mathcal{V}_{\text{train}}$ is the training node set, and \mathbf{y}^j is the ground-truth one-hot label vector of node j .

5 Experiment

In this section, to fully evaluate the performance of the proposed model, we present a series of comprehensive experiments to answer the following research questions (**RQs**):

- **RQ1:** Can the performance of polynomial spectral GNNs be improved by incorporating homophily estimated by LLMs?
- **RQ2:** How does the homophily estimated by LLMs compare to other estimation methods in enhancing polynomial spectral GNNs?
- **RQ3:** Does the LLM-based homophily estimation incur lower inference cost?
- **RQ4:** What is the impact of the key hyperparameter β on model performance?

5.1 Experimental Setup

Datasets. We select ten graph datasets with text attributes, including three citation networks (Cora, Citeseer, and Pubmed), four webpage networks (Cornell, Texas, Washington, and Wisconsin), and three Amazon co-purchase networks (Children, History, and Fitness). These datasets cover both homophilic and heterophilic graph structures. The statistics of these datasets are summarized in Table 2.

Settings. We adopt the experimental setup used in CS-TAG (Yan et al. 2023) and follow its standard data split to ensure a fair comparison. Specifically, the training/validation/test sets are divided as 60%/20%/20% for all datasets except Fitness, for which the split is 20%/10%/70%. We use the accuracy metric as an evaluation indicator. All experiments are performed three times, and we report the average results and their corresponding standard errors. All experiments are conducted on a machine with 3 NVIDIA A5000 24GB GPUs and Intel(R) Xeon(R) Silver 4310 2.10 GHz CPU.

Baselines. To thoroughly evaluate the effectiveness of the proposed method, in addition to the three polynomial spectral GNN backbones—GPR-GNN (Chien et al. 2021), BernNet (He et al. 2021), JacobiConv (Wang and Zhang 2022), and ChebNetII (He, Wei, and Wen 2022)—we also include four classical GNN models and a Multi-Layer Perceptron (MLP) as baselines: GCN (Kipf and Welling 2017), GAT (Veličković et al. 2019), GraphSAGE (Hamilton, Ying, and Leskovec 2017), APPNP (Gasteiger, Bojchevski, and Günnemann 2019), TFE-GNN (Duan et al. 2024), and UniFilter (Huang et al. 2024).

5.2 Main Results (RQ1)

Table 3 presents the node classification results across ten datasets. As observed, the proposed method consistently outperforms GPRGNN, BernNet, JacobiConv, and ChebNetII by a significant margin. Specifically, it achieves an average improvement of 1.14% over GPRGNN, 4.51% over BernNet, 2.51% over JacobiConv, and 2.41% over ChebNetII. These results clearly demonstrate the effectiveness of the proposed method. Moreover, although recent methods such as ChebNetII and TFE-GNN have shown competitive

Table 2: Dataset Statistics

Dataset	Children	History	Fitness	Cornell	Texas	Washington	Wisconsin	Cora	Pubmed	Citeseer
Nodes	76,875	41,551	173,055	191	187	229	265	2,708	19,717	3,186
Edges	1,554,578	358,574	1,773,500	292	310	394	510	10,556	88,648	8,450
Feat	768	768	768	768	768	768	768	1,433	500	3,703
Classes	24	12	13	5	5	5	5	7	3	6
Homophily	0.42	0.66	0.90	0.12	0.06	0.15	0.17	0.81	0.80	0.78

Table 3: Performance (%) on Various Datasets (mean with standard deviation as subscript)

Method	Washington	Wisconsin	Cornell	Texas	Children	History	Fitness	Cora	Citeseer	Pubmed
MLP	80.85 \pm 0.00	84.91 \pm 0.00	68.38 \pm 1.48	79.82 \pm 1.52	54.90 \pm 0.04	83.91 \pm 0.14	79.57 \pm 0.06	79.52 \pm 0.32	71.68 \pm 1.68	87.43 \pm 0.11
GCN	57.45 \pm 4.26	35.85 \pm 3.77	37.61 \pm 10.36	57.02 \pm 1.52	56.47 \pm 0.10	84.82 \pm 0.05	90.86 \pm 0.06	86.22 \pm 0.57	78.58 \pm 0.81	85.02 \pm 0.21
GraphSAGE	78.72 \pm 2.13	78.62 \pm 1.09	69.23 \pm 4.44	76.32 \pm 2.64	54.39 \pm 1.32	84.51 \pm 0.19	88.55 \pm 2.07	86.65 \pm 0.77	76.96 \pm 1.36	88.80 \pm 0.31
GAT	44.68 \pm 11.85	38.36 \pm 4.75	30.77 \pm 10.26	51.75 \pm 15.20	49.78 \pm 4.31	82.79 \pm 1.18	90.51 \pm 0.68	84.93 \pm 0.76	78.16 \pm 0.45	85.04 \pm 0.38
APNP	68.79 \pm 2.45	54.72 \pm 0.00	57.26 \pm 1.48	62.28 \pm 1.52	45.34 \pm 0.27	81.42 \pm 0.07	80.33 \pm 0.36	88.01 \pm 0.64	81.40 \pm 0.33	87.58 \pm 0.03
TFEGNN	68.09 \pm 9.19	72.33 \pm 6.41	66.67 \pm 5.54	64.04 \pm 1.24	45.44 \pm 0.83	81.19 \pm 0.03	83.31 \pm 1.02	85.50 \pm 0.27	77.83 \pm 0.52	88.25 \pm 0.17
UniFilter	88.61 \pm 4.16	84.52 \pm 3.01	69.00 \pm 4.12	79.38 \pm 3.65	47.55 \pm 0.16	86.99 \pm 0.84	87.81 \pm 4.74	87.19 \pm 1.73	77.57 \pm 2.10	85.55 \pm 3.63
GPRGNN	82.98 \pm 2.13	79.87 \pm 4.75	68.38 \pm 2.96	81.58 \pm 2.63	60.29 \pm 0.46	86.03 \pm 0.07	92.38 \pm 0.07	88.01 \pm 0.19	78.16 \pm 0.33	89.11 \pm 0.19
GPRGNNPLUS	87.23\pm0.00	81.76\pm2.18	70.94\pm2.96	83.33\pm1.52	61.00\pm0.20	86.47\pm0.13	92.58\pm0.04	88.07\pm0.21	79.94\pm0.41	89.53\pm0.09
BernNet	79.43 \pm 1.23	84.91 \pm 1.89	67.52 \pm 1.48	80.70 \pm 1.52	58.76 \pm 0.17	84.93 \pm 0.30	91.83 \pm 0.16	82.41 \pm 0.60	72.83 \pm 1.48	88.54 \pm 0.36
BernNetPLUS	90.78\pm1.23	85.53\pm2.18	71.79\pm5.13	83.33\pm1.52	60.80\pm0.19	85.66\pm0.09	92.44\pm0.06	87.58\pm1.06	78.89\pm1.28	89.37\pm0.08
JacobiConv	78.01 \pm 2.45	84.28 \pm 1.09	64.96 \pm 3.92	79.82 \pm 3.04	59.63 \pm 0.46	85.36 \pm 0.13	90.70 \pm 0.17	84.99 \pm 1.01	72.88 \pm 1.13	88.04 \pm 0.10
JacobiConvPLUS	80.85\pm0.00	84.91\pm1.89	68.38\pm1.48	80.70\pm1.52	59.67\pm0.05	85.79\pm0.07	91.04\pm0.26	88.25\pm0.39	78.63\pm1.48	89.48\pm0.13
ChebNetII	82.27 \pm 1.00	85.53 \pm 0.89	68.38 \pm 1.21	84.21 \pm 2.15	56.74 \pm 0.07	84.76 \pm 0.10	83.49 \pm 0.02	81.01 \pm 0.12	72.37 \pm 0.24	88.34 \pm 0.13
ChebNetIPLUS	87.94\pm1.00	85.53\pm0.89	69.23\pm2.09	84.21\pm2.15	58.76\pm0.12	85.79\pm0.05	88.22\pm0.17	83.53\pm0.17	74.12\pm0.36	88.34\pm0.10

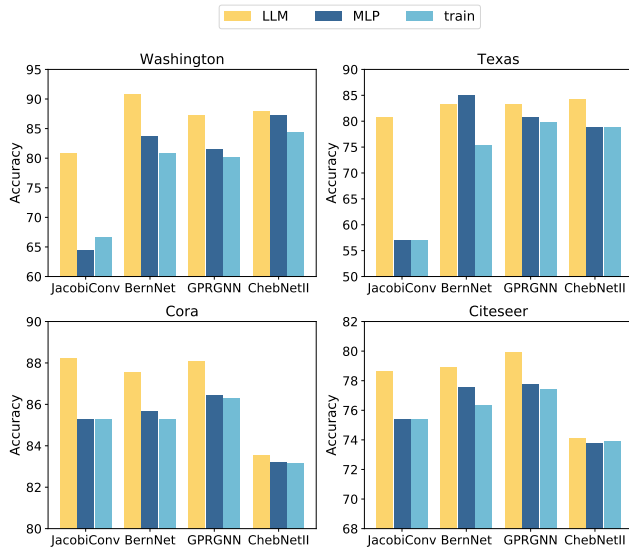


Figure 2: Ablation study of proposed method.

performance, our method still surpasses them. This highlights the strong representational power of LLM-enhanced spectral GNNs.

5.3 Ablation Analysis (RQ2)

This subsection aims to evaluate the advantage of using LLM-predicted homophily in polynomial spectral GNNs. We consider the following two alternative variants for com-

parison:

1. Training a MLP to predict homophily and enhance the spectral GNN.
2. Directly using the homophily computed from the training set to enhance the spectral GNN.

Figure 2 compares the performance of spectral GNNs enhanced with homophily estimated by different methods on four datasets¹. As shown, the homophily predicted by LLMs yields the best performance in nearly all cases, with the only exception being BernNet on the Texas dataset. This demonstrates the superiority of LLM-estimated homophily over that derived from MLPs or directly from the training set, likely due to the stronger reasoning capability of LLMs. In addition, MLP-based homophily estimation generally outperforms the one directly obtained from the training set, indicating that learning homophily via a trainable model is more effective than relying on limited labeled data. However, MLP-based variants still fall short of the LLM-based approach, highlighting that stronger models can generate more informative homophily signals, which in turn lead to better performance when integrated into spectral GNNs.

5.4 Efficiency Studies (RQ3)

To evaluate the efficiency of the proposed method, we measure both its monetary cost and time overhead. Since our method employs low-cost GPT-4o Mini API calls to estimate homophily levels on different datasets, a small monetary expense is incurred. Table 4 reports the input, output, and total monetary cost per dataset. As shown, the cost

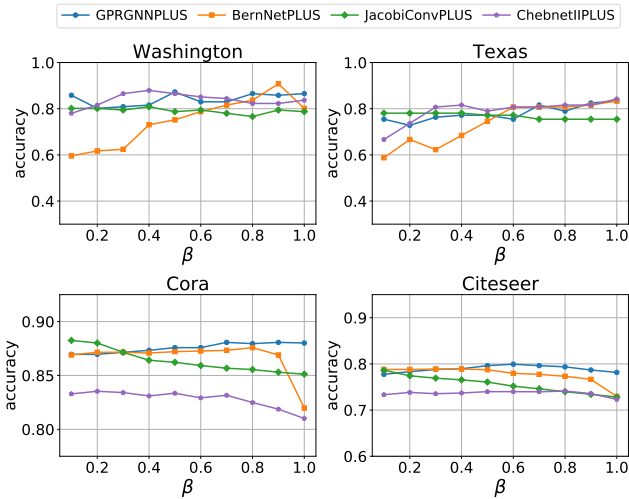
¹Please refer to Appendix B for more results.

Table 4: Token and cost statistics on each dataset (million tokens / USD)

Type	Washington	Wisconsin	Cornell	Texas	Children	History	Fitness	Cora	Citeseer	Pubmed
Output	0.12M/0.07\$	0.13M/0.08\$	0.14M/0.09\$	0.13M/0.08\$	0.17M/0.10\$	0.16M/0.10\$	0.15M/0.09\$	0.17M/0.10\$	0.16M/0.10\$	0.18M/0.11\$
Input	0.47M/0.07\$	0.67M/0.10\$	0.56M/0.08\$	0.44M/0.07\$	0.38M/0.06\$	0.36M/0.05\$	0.09M/0.01\$	0.22M/0.03\$	0.24M/0.04\$	0.40M/0.06\$
Total	0.59M/0.14\$	0.80M/0.18\$	0.71M/0.17\$	0.57M/0.14\$	0.55M/0.16\$	0.53M/0.15\$	0.24M/0.10\$	0.39M/0.13\$	0.40M/0.13\$	0.58M/0.17\$

Table 5: Per-epoch training time (ms) and total training time (s) comparisons on various datasets.

Method	Washington	Wisconsin	Cornell	Texas	Children	History	Fitness	Cora	Citeseer	Pubmed
GPRGNN	13.00/2.60	12.30/2.46	11.80/2.36	13.40/2.67	230.80/46.16	94.90/18.97	472.70/94.54	15.00/3.00	31.40/6.29	32.60/6.52
GPRGNNPLUS	13.60/2.72	14.00/2.81	13.90/2.77	13.90/2.78	274.00/54.80	119.10/23.83	575.40/115.08	18.80/3.76	41.40/8.28	40.60/8.12
BernNet	37.50/7.50	36.90/7.38	38.60/7.72	35.90/7.18	1235.30/247.06	445.70/89.15	2449.40/489.88	50.20/10.04	132.10/26.42	128.30/25.67
BernNetPLUS	43.50/8.69	40.90/8.17	43.80/8.76	43.50/8.71	1303.50/260.70	473.80/94.77	2596.20/519.23	53.70/10.73	143.10/28.63	138.20/27.65
JacobiConv	26.80/5.36	26.80/5.36	26.80/5.36	26.80/5.35	56.80/11.37	33.90/6.77	88.00/17.60	28.80/5.76	28.10/5.63	30.10/6.02
JacobiConvPLUS	28.10/5.63	28.60/5.72	27.90/5.58	28.00/5.59	56.50/11.31	34.40/6.88	86.30/17.26	30.50/6.09	29.80/5.96	31.30/6.26
ChebNetII	49.40/9.88	50.20/10.05	49.60/9.93	49.20/9.83	274.70/54.95	137.00/27.41	574.50/114.89	51.80/10.35	70.40/14.08	68.80/13.76
ChebNetIPLUS	50.00/10.01	50.70/10.13	50.60/10.12	51.20/10.24	324.20/64.84	164.50/32.90	685.70/137.13	54.80/10.95	79.50/15.89	76.90/15.38

Figure 3: Effect of hyperparameter β on model performance.

for each dataset ² remains below \$0.2, indicating that our method achieves high model performance at a minimal financial expense.

To further assess the time efficiency of our approach, we compare the per-epoch and total training time with those of the original polynomial spectral GNNs. As shown in Table 5, the runtime of our method remains similar to the original GNNs across all ten datasets, suggesting that the proposed approach does not increase time complexity.

In practice, the only additional computation introduced by the proposed method, compared to standard spectral GNNs, lies in the construction of heterophily-aware basis functions based on the predicted homophily levels. This step is shared across all graph convolution layers and can thus be pre-computed for different polynomial orders. During training, the precomputed basis vectors can be directly loaded to significantly reduce computational overhead. Furthermore, it

²Please refer to Appendix C for hyperparameter sensitivity results on additional datasets.

is worth emphasizing that our approach does not rely on costly fine-tuning or local model deployment, highlighting both the efficiency and practical applicability of the proposed method.

5.5 Parameter Sensitivity Analysis (RQ4)

In the Methodology Section, we introduce a key hyperparameter β to balance the contribution between the original polynomial basis and the heterophily-aware basis constructed using predicted homophily. A lower value of β indicates a greater reliance on the heterophily-aware basis, while a higher β emphasizes the original polynomial basis. Figure 3 illustrates the sensitivity of hyperparameter β on four datasets. As shown, different polynomial models exhibit distinct trends depending on the dataset. For example, BernNetPLUS demonstrates an upward trend in the Washington and Texas datasets. This may be attributed to BernNet’s strong capacity to approximate arbitrary filters, making the original polynomial basis more influential. In contrast, GPRGNNPLUS and JacobiConvPLUS appear largely insensitive to changes in β , suggesting that both the original and heterophily-aware bases are equally effective at capturing meaningful filters. Conversely, on the Cora and Citeseer datasets, all three models show a generally decreasing trend, indicating that for homophilic graphs, incorporating more heterophily-aware basis functions—constructed based on predicted homophily—can lead to improved performance.

6 Conclusion

This paper is the first to investigate the potential of LLMs in enhancing spectral GNNs. We propose a novel framework that utilizes LLM-predicted homophily to construct a heterophily basis, which is then integrated into existing spectral GNN architectures. The approach begins by sampling a subset of edges from the graph and employing an LLM to infer whether connected node pairs belong to the same class, thereby estimating homophily. This estimated homophily guides the construction of a heterophily-aware

representation, enabling spectral GNNs to handle both homophilic and heterophilic graphs better.

Extensive experiments on multiple benchmark datasets demonstrate that our method consistently improves the performance of various spectral GNNs, while incurring minimal computational and monetary overhead. These results highlight the promising synergy between LLMs and spectral graph learning, and open up new directions for future research at the intersection of language models and graph neural architectures.

References

- Achiam, J.; Adler, S.; Agarwal, S.; Ahmad, L.; Akkaya, I.; Aleman, F. L.; Almeida, D.; Altenschmidt, J.; Altman, S.; Anadkat, S.; et al. 2023. Gpt-4 technical report. *arXiv preprint arXiv:2303.08774*.
- Bo, D.; Shi, C.; Wang, L.; and Liao, R. 2023. Specformer: Spectral Graph Neural Networks Meet Transformers. In *The Eleventh International Conference on Learning Representations*.
- Cappuzzo, R.; Papotti, P.; and Thirumuruganathan, S. 2020. Creating embeddings of heterogeneous relational datasets for data integration tasks. In *Proceedings of the 2020 ACM SIGMOD international conference on management of data*, 1335–1349.
- Chen, Z.; Chen, F.; Zhang, L.; Ji, T.; Fu, K.; Zhao, L.; Chen, F.; Wu, L.; Aggarwal, C.; and Lu, C.-T. 2023a. Bridging the gap between spatial and spectral domains: A unified framework for graph neural networks. *ACM Computing Surveys*, 56(5): 1–42.
- Chen, Z.; Mao, H.; Wen, H.; Han, H.; Jin, W.; Zhang, H.; Liu, H.; and Tang, J. 2023b. Label-free node classification on graphs with large language models (llms). *arXiv preprint arXiv:2310.04668*.
- Chien, E.; Peng, J.; Li, P.; and Milenkovic, O. 2021. Adaptive Universal Generalized PageRank Graph Neural Network. In *International Conference on Learning Representations*.
- Defferrard, M.; Bresson, X.; and Vandergheynst, P. 2016. Convolutional neural networks on graphs with fast localized spectral filtering. *Advances in neural information processing systems*, 29.
- Duan, R.; Guang, M.; Wang, J.; Yan, C.; Qi, H.; Su, W.; Tian, C.; and Yang, H. 2024. Unifying Homophily and Heterophily for Spectral Graph Neural Networks via Triple Filter Ensembles. *Advances in Neural Information Processing Systems*, 37: 93540–93567.
- Gao, C.; Zheng, Y.; Li, N.; Li, Y.; Qin, Y.; Piao, J.; Quan, Y.; Chang, J.; Jin, D.; He, X.; et al. 2023. A survey of graph neural networks for recommender systems: Challenges, methods, and directions. *ACM Transactions on Recommender Systems*, 1(1): 1–51.
- Gasteiger, J.; Bojchevski, A.; and Günnemann, S. 2019. Predict then Propagate: Graph Neural Networks meet Personalized PageRank. In *International Conference on Learning Representations*.
- Guo, J.; Huang, K.; Yi, X.; and Zhang, R. 2023. Graph neural networks with diverse spectral filtering. In *Proceedings of the ACM Web Conference 2023*, 306–316.
- Guo, Z.; Xia, L.; Yu, Y.; Wang, Y.; Yang, Z.; Wei, W.; Pang, L.; Chua, T.-S.; and Huang, C. 2024. Graphedit: Large language models for graph structure learning. *arXiv preprint arXiv:2402.15183*.
- Hamilton, W.; Ying, Z.; and Leskovec, J. 2017. Inductive representation learning on large graphs. *Advances in neural information processing systems*, 30.
- He, M.; Wei, Z.; and Wen, J.-R. 2022. Convolutional neural networks on graphs with chebyshev approximation, revisited. *Advances in Neural Information Processing Systems*, 35: 7264–7276.
- He, M.; Wei, Z.; Xu, H.; et al. 2021. Bernnet: Learning arbitrary graph spectral filters via bernstein approximation. *Advances in Neural Information Processing Systems*, 34: 14239–14251.
- He, X.; Bresson, X.; Laurent, T.; Perold, A.; LeCun, Y.; and Hooi, B. 2024. Harnessing Explanations: LLM-to-LM Interpreter for Enhanced Text-Attributed Graph Representation Learning. In *The Twelfth International Conference on Learning Representations*.
- Hu, J.; Guo, C.; Yang, B.; and Jensen, C. S. 2019. Stochastic weight completion for road networks using graph convolutional networks. In *2019 IEEE 35th international conference on data engineering (ICDE)*, 1274–1285. IEEE.
- Huang, C.; Fang, Y.; Lin, X.; Cao, X.; Zhang, W.; and Orłowska, M. 2022. Estimating node importance values in heterogeneous information networks. In *2022 IEEE 38th International Conference on Data Engineering (ICDE)*, 846–858. IEEE.
- Huang, K.; Wang, Y. G.; Li, M.; et al. 2024. How universal polynomial bases enhance spectral graph neural networks: Heterophily, over-smoothing, and over-squashing. *arXiv preprint arXiv:2405.12474*.
- Jiang, W.; and Luo, J. 2022. Graph neural network for traffic forecasting: A survey. *Expert systems with applications*, 207: 117921.
- Kipf, T. N.; and Welling, M. 2017. Semi-Supervised Classification with Graph Convolutional Networks. In *International Conference on Learning Representations*.
- Ling, C.; Li, Z.; Hu, Y.; Zhang, Z.; Liu, Z.; Zheng, S.; and Zhao, L. 2024. Link Prediction on Textual Edge Graphs. *arXiv preprint arXiv:2405.16606*.
- Ren, X.; Tang, J.; Yin, D.; Chawla, N.; and Huang, C. 2024. A survey of large language models for graphs. In *Proceedings of the 30th ACM SIGKDD Conference on Knowledge Discovery and Data Mining*, 6616–6626.
- Sharma, K.; Lee, Y.-C.; Nambi, S.; Salian, A.; Shah, S.; Kim, S.-W.; and Kumar, S. 2024. A survey of graph neural networks for social recommender systems. *ACM Computing Surveys*, 56(10): 1–34.
- Sun, S.; Ren, Y.; Ma, C.; and Zhang, X. 2023. Large language models as topological structure enhancers for text-attributed graphs. *arXiv preprint arXiv:2311.14324*.

Tang, J.; Hua, F.; Gao, Z.; Zhao, P.; and Li, J. 2024a. Gadbench: Revisiting and benchmarking supervised graph anomaly detection. *Advances in Neural Information Processing Systems*, 36.

Tang, J.; Li, J.; Gao, Z.; and Li, J. 2022. Rethinking graph neural networks for anomaly detection. In *International Conference on Machine Learning*, 21076–21089. PMLR.

Tang, J.; Yang, Y.; Wei, W.; Shi, L.; Su, L.; Cheng, S.; Yin, D.; and Huang, C. 2024b. Graphgpt: Graph instruction tuning for large language models. In *Proceedings of the 47th International ACM SIGIR Conference on Research and Development in Information Retrieval*, 491–500.

Veličković, P.; Cucurull, G.; Casanova, A.; Romero, A.; Liò, P.; and Bengio, Y. 2019. Graph Attention Networks. In *International Conference on Learning Representations*.

Wang, X.; and Zhang, M. 2022. How powerful are spectral graph neural networks. In *International Conference on Machine Learning*, 23341–23362. PMLR.

Wu, J.; Gan, W.; Chen, Z.; Wan, S.; and Yu, P. S. 2023. Multimodal large language models: A survey. In *2023 IEEE International Conference on Big Data (BigData)*, 2247–2256. IEEE.

Wu, Y.; Li, S.; Fang, Y.; and Shi, C. 2024. Exploring the Potential of Large Language Models for Heterophilic Graphs. *arXiv preprint arXiv:2408.14134*.

Xie, H.; Zheng, D.; Ma, J.; Zhang, H.; Ioannidis, V. N.; Song, X.; Ping, Q.; Wang, S.; Yang, C.; Xu, Y.; et al. 2023. Graph-aware language model pre-training on a large graph corpus can help multiple graph applications. In *Proceedings of the 29th ACM SIGKDD Conference on Knowledge Discovery and Data Mining*, 5270–5281.

Yan, H.; Li, C.; Long, R.; Yan, C.; Zhao, J.; Zhuang, W.; Yin, J.; Zhang, P.; Han, W.; Sun, H.; et al. 2023. A comprehensive study on text-attributed graphs: Benchmarking and rethinking. *Advances in Neural Information Processing Systems*, 36: 17238–17264.

Zhang, M.; Sun, M.; Wang, P.; Fan, S.; Mo, Y.; Xu, X.; Liu, H.; Yang, C.; and Shi, C. 2024a. GraphTranslator: Aligning Graph Model to Large Language Model for Open-ended Tasks. In *Proceedings of the ACM on Web Conference 2024*, 1003–1014.

Zhang, Z.; Wang, X.; Zhou, H.; Yu, Y.; Zhang, M.; Yang, C.; and Shi, C. 2024b. Can Large Language Models Improve the Adversarial Robustness of Graph Neural Networks? *arXiv preprint arXiv:2408.08685*.

Zhao, W. X.; Zhou, K.; Li, J.; Tang, T.; Wang, X.; Hou, Y.; Min, Y.; Zhang, B.; Zhang, J.; Dong, Z.; et al. 2023. A survey of large language models. *arXiv preprint arXiv:2303.18223*, 1(2).

Zhu, J.; Yan, Y.; Zhao, L.; Heimann, M.; Akoglu, L.; and Koutra, D. 2020. Beyond homophily in graph neural networks: Current limitations and effective designs. *Advances in neural information processing systems*, 33: 7793–7804.